

Anaam A. Sabri

Department of Chemical Engineering, University of Technology, 52 Alsinaa St., Baghdad, Iraq.

aaksabri@yahoo.com**Noor S. Abbood** 

Department of Chemical Engineering, University of Technology, 52 Alsinaa St., Baghdad, Iraq.

Received on: 29/09/2018

Accepted on: 24/02/2019

Published online: 25/04/2019

Adsorption Study of Nitrate Anions by Different Materials Using Fixed Bed Column

Abstract- MCM-41 is, a mesoporous material with a hexagonal structure, has a high surface area, high pore vol., and low mass density. Continuous adsorption fixed bed of $\text{NH}_2\text{-MCM-41}$ adsorbent was utilized for the removal of nitrate anions from aqueous solutions. The effect of adsorbent weight (0.5, 1, 2 gm), flow rate (0.5, 1.0, 1.5 ml/min) and initial NO_3^- concentrations (50, 75, 100 mg/l) on breakthrough curves were studied. It was found that breakthrough time increases with increasing column bed height and decreases with increasing NO_3^- inlet concentration and flow rate. The highest removal percentage (75.2%) achieved at inlet concentration of 100 mg/L of NO_3^- anion, 1gm adsorbent weight and 1.5 mL/min flow rate. Thomas and Yan adsorption models showed a good fit to the experimental data. Removal of nitrate anion by traditional activated carbon was also investigated and the results were compared with the nitrate removal by $\text{NH}_2\text{-MCM-41}$. It was concluded that $\text{NH}_2\text{-MCM-41}$ is more efficient in nitrate removal than activated carbon and the maximum removal percentage of nitrate anions by traditional activated carbon was found to be 55.8%.

Keywords- fixed bed, nitrate anion, $\text{NH}_2\text{-MCM-4}$.

How to cite this article: A.A. Sabri and N.S. Abbood, "Adsorption Study of Nitrate Anions by Different Materials Using Fixed Bed Column," *Engineering and Technology Journal*, Vol. 37, Part C, No. 1, pp. 156-162, 2019.

1. Introduction

The nitrate ion is of prime importance on a worldwide scale. Because of its high water solubility, all sources of aqueous nitrogen tend to be changed over to nitrate. Furthermore is potentially the most general groundwater contaminant on the planet, distinguishing a significant danger to drinking water supplying and advancing eutrophication [1, 2, 3]. Eutrophication is when a body of water becomes overly enriched with minerals and nutrients that induce excessive growth of plants and algae; this process may result in oxygen depletion of the water body [4]. Nitrate concentration over the most extreme admissible point in drinking water is damaging to human well-being. Nitrate exposure can additionally prompt a few medical problems, for example, a blue disease in babies called methemoglobinemia, diabetes, birth defects, vomiting, stomach pain, changes in the immunity system, diarrhea [1, 3]. To restrain the hazard to human well-being from nitrate in drinkable, the World Health Organization (WHO) and the European Community (EC) have settled the Maximum Contaminant Levels (MCL) at 11.3 mg NO_3^-/L (50 mg NO_3^-/L) [5]. Numerous conventional techniques have been employed to remove nitrate from wastewater. These techniques incorporate chemical methods [6], biological de-nitrification [7, 8, 9], and physical methods [10]. Elimination of nitrate by the

adsorption method has pulled in much consideration, which are simple and inexpensive operations; they produce little sludge and permit nitrate recovery [11]. Actual adsorption processes are mostly associated with adsorption in a column. Adsorbent particles were packed in a column and liquid that contains at least one constituent of adsorbates flows down through the packed bed. Adsorption occurs from the inlet of the column and continues to the exit [2].

The mass transfer zone (MTZ) is defined as the surface of the bed which is active and adsorption takes place on it Fig.1 [2], the liquid flowing into the column from the top and the adsorbent rapidly adsorbs the contaminant as it contacts with the liquid. In this way, the liquid leaving the column is free of contaminant. If concentrations in the effluent stream are estimated constantly, leakage of the absorbable constituents are noticed when the mass transfer zone approaches the exit of the bed and the "breakthrough curve" will be obtained [12].

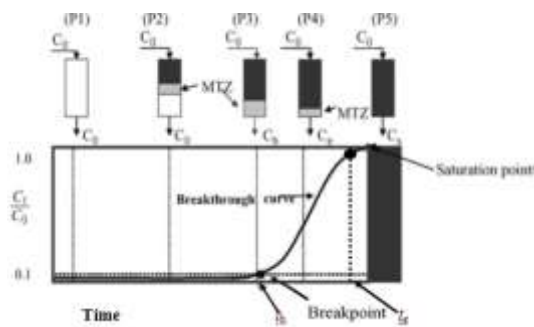


Figure 1: Typical breakthrough curve showing the movement of the mass transfer zone [2]

A breakthrough curve is a plot of the column effluent concentration as a function of either the volume treated or the time of treatment. A perfect breakthrough curve is the S-shape. The state of the breakthrough curve is subject to a few parameters, including the feed concentration, the feed flow rate, the height, shape, and kind of adsorbent, and the temperature or pressure of the system [13]. The breakthrough and exhausted time, t_b and t_e , separately are estimated in the breakthrough curve as appeared in Figure 1. The breakthrough time demonstrates the moment in which the contaminant is successfully released on effluent and determined just as the concentration (C_e) gets to about five percent of the (C_o) that depicts the time which the bed is yet effective. When the concentration (C_o) surpasses ninety-five percent of that in (C_e), the exhaustion time (t_e) is established indicating the time which the bed is exhausted.

2. Fixed bed column data analysis

For an optical outline of an industrial adsorption process, the examination of the adsorption experimental information is essential. From the proportion of mass adsorbate (q_{total}) to the total sum of adsorbate sent to the column (m_{total}), the total adsorbate removal percent can be computed, which can be resolved from [8]:

$$R\% = \frac{q_{total}}{m_{total}} * 100 \quad (1)$$

The total mass of adsorbate adsorbed (q_{total} , mg) can be determined by:

$$q_{total} = \frac{Q * C_o}{1000} \int_{t=0}^{t=t_{total}} \left(1 - \frac{C_e}{C_o}\right) dt \quad (2)$$

where:

Q the flow rate (ml/min) that can be calculated by dividing the effluent volume (V_{eff} , ml) by the total time (t_{total} , min.).

$$Q = \frac{V_{eff}}{t_{total}} \quad (3)$$

Besides, the total sum of adsorbate went through the column (mg) can be ascertained from the accompanying articulation:

$$m_{total} = \frac{C_o * t_e * Q}{1000} \quad (4)$$

The equilibrium adsorption capacity q_e (mg/g) can be computed utilizing the accompanying condition:

$$q_e = \frac{q_{total}}{m} \quad (5)$$

Where m is the weight of adsorbent (g).

3. Fixed Bed Column Data Modeling

I. Thomas model

The adsorption capacity of the adsorbent can be computed by this model, which is useful in the successful design of the adsorption procedure [14]. The nonlinear articulation of Thomas display for fixed bed adsorption is given as [15]:

$$\frac{C_e}{C_o} = \frac{1}{1 + \exp\left[\left(\frac{k_{th}q_{th}m}{Q}\right) - k_{th}C_o t\right]} \quad (6)$$

Where:

K_{th} : kinetic adsorption rate constant for Thomas model (ml/mg.min).

q_{th} : maximum adsorption capacity estimated by Thomas model (mg/g).

t : time in min.

Eq. (6) can be composed as the accompanying structure:

$$\ln\left(\frac{C_o}{C_e} - 1\right) = \frac{k_{th}q_{th}m}{Q} - k_{th}C_o t \quad (7)$$

Thomas parameters k_{th} and q_{th} can be resolved utilizing nonlinear relapse by plotting $\ln\left(\frac{C_o}{C_e} - 1\right)$ versus t .

II. Yan model

An empirical condition proposed which could defeat the disadvantage in Thomas model particularly its important insufficiency in anticipating the effluent concentration concerning time zero. The observational condition proposed by Yan has discovered a better description of the breakthrough curves in a fixed bed column. This condition is communicated as takes after [9]:

$$\frac{C_e}{C_o} = 1 - \frac{1}{1 + \left(\frac{C_o Q t}{q_y m}\right)^a} \quad (8)$$

where:

a : constant of Yan model.

q_y : maximum adsorption by the adsorbent (mg/g) estimated by Yan model.

Eq. (8) can be examined as the accompanying structure:

$$\ln\left(\frac{C_e}{C_o - C_e}\right) = a \ln t - a \ln \frac{q_y m}{C_o Q} \quad (9)$$

Yan model constants (a , q_y) can be acquired from the plot of $\ln\left(\frac{C_e}{C_o - C_e}\right)$ against $\ln t$.

4. Experimental Work

I. Materials

Sodium nitrate (NaNO_3) 99% purity for stock solution of nitrate solution, $\text{NH}_2\text{-MCM-41}$ which was prepared as in previous work [17] using tetraethyl orthosilicate (TEOS) 98% purity as a source of silicate and cetyltrimethylammonium bromide (CTAB) 98% purity as a template then functionalized by 3-aminopropyltriethoxysilane (APTES) 98% purity.

II. Experiments of Fixed Bed Column

In the fixed bed column experiment a cylindrical glass column with a diameter of (1.6 cm) and (50 cm) height was used. Various heights of $\text{NH}_2\text{-MCM-41}$ were packed in the column that is supported from the bottom with glass wool. To pump a solution containing the NO_3^- anion from a vessel of size 500 ml to the top of the column in a continuous process, a peristaltic pump [Type: BT100-1F Hebei, Origin: China] was used. And the specimens were taken from the base of the column at interim of time. Figure 2 demonstrates the schematic chart of the procedure. Adsorption tests were done at different weights (0.5, 1, 2 gm) of [$\text{NH}_2\text{-MCM-41}$ and activated carbon], various flow rates (0.5, 1.0, and 1.5) ml/min and various concentrations of NO_3^- anion (50, 75, and 100) mg/L on certain pH and room temp., in an attempt to acquire the best conditions for the packed bed column.

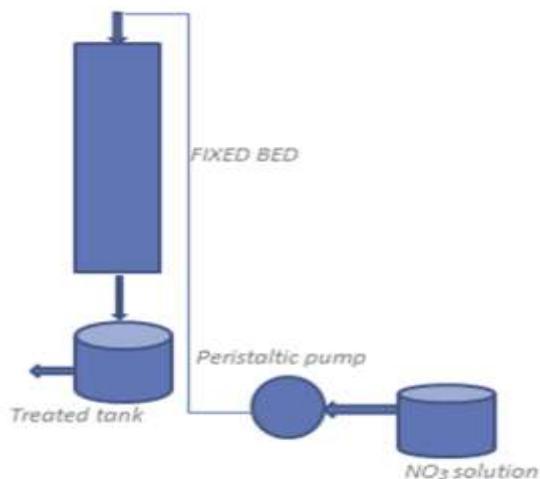


Figure 2: Schematic diagram of a continuous fixed bed process.

5. Results and Discussions

I. Effect of adsorbent weight

The quantity of adsorbent inside the fixed bed column mainly controls the agglomeration of NO_3^- anion in the column. Figure 3 displays the adsorption breakthrough curves at two weights (0.5, 1gm) of $\text{NH}_2\text{-MCM-41}$ for examined nitrate anion. It was noticed that as the weight of adsorbent was increased, the removal percent of NO_3^- anion also increased as revealed in Table 1. Additionally, with increasing the weight of $\text{NH}_2\text{-MCM-41}$ from 0.5 to 1 gm, the breakthrough time were observed to be increased from 53 to 100min; and the exhaust time were observed to be increased from 121 to 164min., that produced the highest removal percent of NO_3^- anion. Due to the transfer area needs extra opportunity to attain the end of the column for the NO_3^- to be in contact with $\text{NH}_2\text{-MCM-41}$. Furthermore, due to the extra amount of binding sites for the adsorption process.

Additionally, the results in Table 1 show that the point at which the weight is 0.5 gm has the maximum q_e . This showing that the q_e wasn't specifically corresponding to the quantity of adsorbent available in the bed, or maybe the amount of $\text{NH}_2\text{-MCM-41}$ at the 1.5 gm bed depth was excessively to use all its ability for this situation ($Q=1.5$ ml/min, $C_0=50$ mg/L). When the bed height increased to 2gm, the nitrate solution could not flow through the bed and accumulate above the bed, because of the transformation of MCM-41 to a substance similar to an emulsion that prevents the nitrate solution to pass through it. As shown in Figure 4, the beads were used with MCM-41 to increase the porosity of the bed and also to prevent the accumulation of nitrate solution above the bed and not to descend from the bottom of the column. Although; the beads have increased the porosity but, they caused the formation of channels inside the bed which, minimizes the removal of the nitrate ion.

The effect of adsorbent weight was also investigated using activated carbon as an adsorbent. Figure 5 represents the breakthrough curves of activated carbon at various weights. The results show the same behavior as $\text{NH}_2\text{-MCM-41}$, but the removal percent, exhaust time, and the breakthrough time were lower than that of $\text{NH}_2\text{-MCM-41}$, as can be seen in Table 2. The maximum adsorption capacity was 7.158mg/g when using a weight of 0.5 gm while the maximum removal percent was 45.1% at weight of 1.5gm.

Table 1: The breakthrough evaluated variables for NH₂-MCM-41 in fixed bed.

L (cm)	Q (ml/min)	conc. (mg/L)	q _e (mg/g)	R%	t _b (min.)	t _e (min.)
1.5 (0.5g)	1.5	50	11.7146	55.9	53	121
1.5 (0.5g)	1.0	50	11.108	61.5	71	160
1.5 (0.5g)	0.5	50	6.7166	66.4	93	180
3 (1g)	1.5	50	9.5377	62.8	100	164
3 (1g)	1.5	75	10.8152	61.4	75	140
3 (1g)	1.5	100	12.7244	75.2	55	120

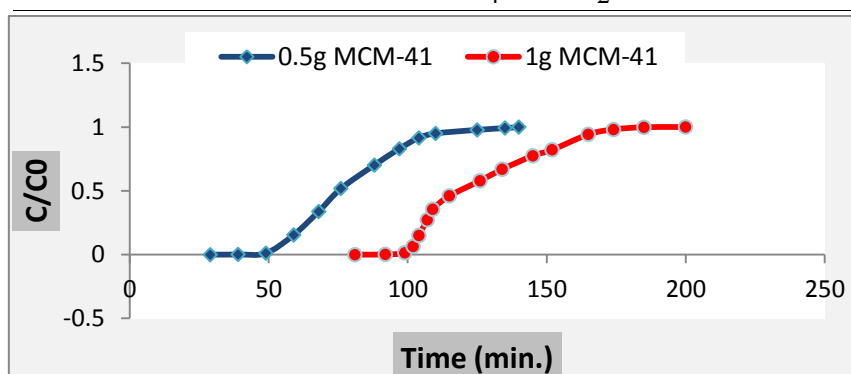


Figure 3: Breakthrough curves of NO₃⁻ adsorption by different weights of NH₂-MCM-41 (C₀=50 mg/l, Q=1.5 ml/min).

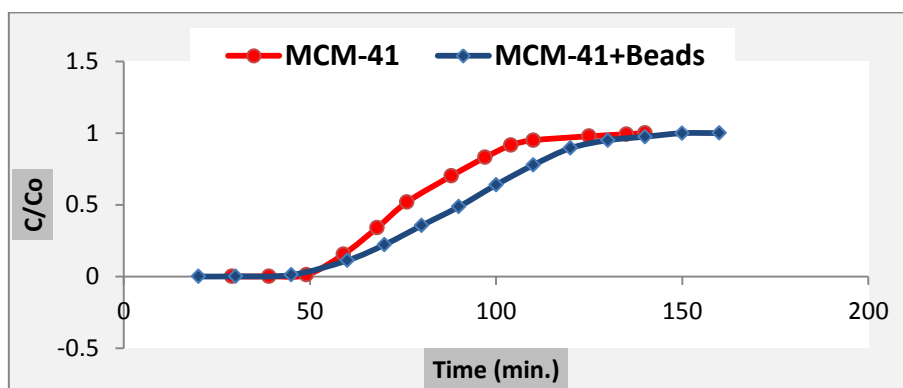


Figure 4: Comparison between MCM-41 and [MCM-41+beads] in fixed bed (Q=1.5ml/min., C₀=50mg/L and dose of adsorbent=1g).

Table 2: The breakthrough investigated parameters for activated carbon.

L (cm)	Q (ml/min)	conc. (mg/L)	q _e (mg/g)	R%	t _b (min.)	t _e (min.)
2 (0.5g)	1.5	50	7.158	44.6	25	73
3 (1g)	1.5	50	4.8515	43.8	40	93
4 (1.5g)	1.5	50	3.4518	45.1	45	115
2 (0.5g)	0.5	50	3.0602	44.2	32	95
2 (0.5g)	1.0	50	6.4628	52.7	37	95
3 (1g)	1.5	75	7.2555	55.8	38	100
3 (1g)	1.5	100	7.0326	43.9	29	75

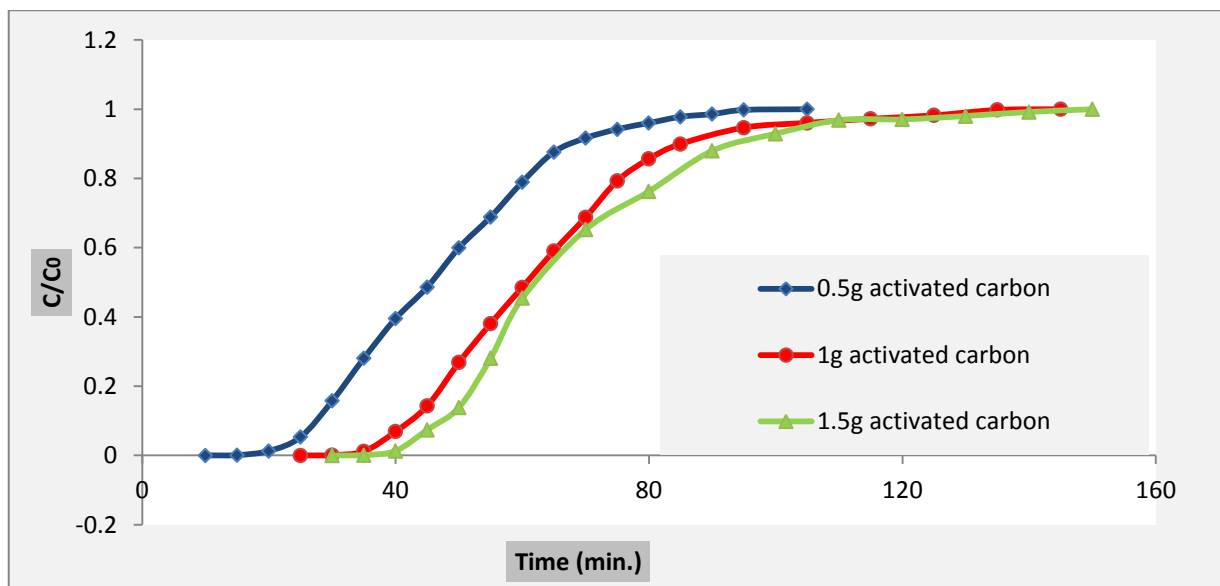


Figure 5: Breakthrough curves for NO_3^- adsorption by activated carbon at different weights ($C_0=50$ mg/l, $Q=1.5$ ml/min).

II. Effect of flow rate

Figure 6 gives the breakthrough curves of NO_3^- anion with different flow rates and the achievement examination is listed in Table 1. The outcomes demonstrate that the breakthrough curves shift towards a lower time scale with increasing the flow rate from 0.5 to 1.5 ml/min at constant bed height and concentration. As the flow rate increases the breakthrough time & the exhaustion time decrease (Table1), neither all the NO_3^- anions will have sufficient time to enter from the sol. To the $\text{NH}_2\text{-MCM-41}$ pores and tie with (NH_2) groups, that produces a lower R% (from 66.4% to 55.9%) of NO_3^- anion in the column (Table 1), since the NO_3^- anions will leave the column before the balance happened .

As opposed to adsorbent weight results, with increasing the flow rate (from 0.5 to 1.5ml/min.) the exhaustion time decreased (from 180 to 121min.). This conduct could clarify that NO_3^- adsorption with $\text{NH}_2\text{-MCM-41}$ is affected by the residence time of the nitrate ions in the column [2, 14, 20]. It is additionally noticed that most extreme nitrate up-take was 11.7146 mg/g at 1.5 ml/min. (Table 1).

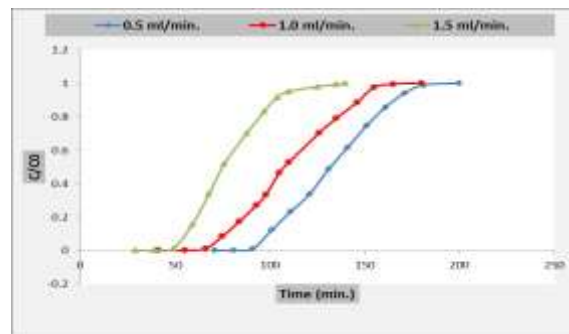


Figure 6: Breakthrough curves for NO_3^- adsorption on $\text{NH}_2\text{-MCM-41}$ at different flow rates ($C_0=50$ mg/l, $L=1.5$ cm).

The impact of flow rate was also examined utilizing activated carbon as an adsorbent for the removal of NO_3^- anion with different flow rates; the breakthrough curves appeared in Figure 7. The results reveal that the behavior of activated carbon was similar to that of $\text{NH}_2\text{-MCM-41}$, but the first was less effective. It was noticed that by increasing the flow rate from 0.5 to 1.5ml/min., the removal percent increased slightly from 44.2% to 44.6%. Also, the exhaustion time decreased from 95 to 73min. When the flow rate increased from 0.5 to 1.5ml/min, and the breakthrough time decreased from 32 to 25min., (Table 2). Additionally, the maximum adsorption capacity was 7.158mg/g at a flow rate of 1.5ml/min.

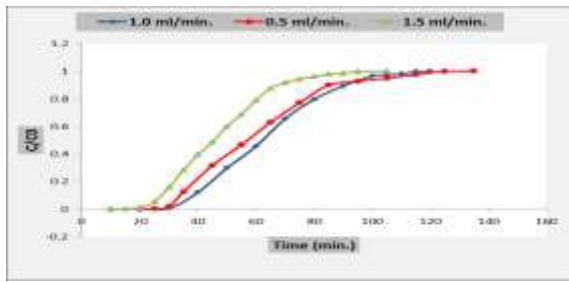


Figure 7: Breakthrough curves for NO_3^- adsorption on activated carbon with different flow rates ($C_0=50 \text{ mg/l}$, $L=2 \text{ cm}$).

III. Effect of the initial concentration of NO_3^-

Utilizing different concentrations of (50, 75, and 100 mg/L) at a flow rate of 1.5 ml/min and a bed height of 3cm, the impact of initial concentration on the adsorption of NO_3^- anion was examined; these curves are shown in Fig.8. It was observed from Fig.8, a reduced initial concentration of nitrate ions gave the longer time required to saturate $\text{NH}_2\text{-MCM-41}$ bed. The breakthrough variables of various nitrate anion concentrations are recorded in Table1. With initial nitrate concentration of 100 mg/L the maximum adsorption capacity (12.7244 mg/g) was gotten, while the higher removal percent was 75.2% at the same initial concentration of NO_3^- anion. The variance amid the concentration of NO_3^- on the solid phase and liquid phase is regarded as the driving force [15]. In this manner, preferable NO_3^- up-take produced if nitrate concentration is high.

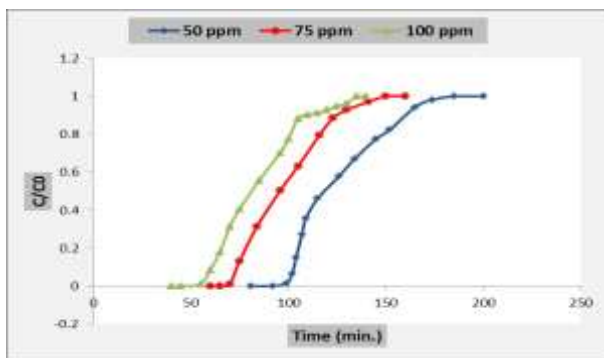


Figure 8: Breakthrough curves for NO_3^- adsorption on $\text{NH}_2\text{-MCM-41}$ with different NO_3^- anion concentrations ($Q=1.5\text{ml/min}$, $L=3 \text{ cm}$).

The impact of the initial concentration of NO_3^- anion was also evaluated using activated carbon, and the breakthrough curves are shown in Fig.9. The results obtained for $\text{NH}_2\text{-MCM-41}$ could be occluded to that of activated carbon. However; the adsorption capacity for activated carbon was low and so as the removal percent (Table2).

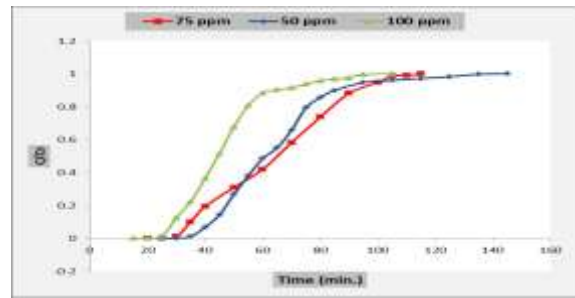


Figure 9: Breakthrough curves of NO_3^- adsorption on activated carbon at different NO_3^- concentrations ($Q=1.5\text{ml/min}$, $L=3 \text{ cm}$).

IV. Column Dynamic Models

Numerical models Thomas [Eq. 7] and Yan [Eq. 9] models were fitted well to the breakthrough curves obtained with different initial nitrate concentrations, and depending on the fitting results the adsorption capacity was estimated. To modify the extreme solid phase concentration (q_{Th}), the experimental data were fitted to both models. The variables of Thomas and Yan models and the breakthrough investigation of $\text{NH}_2\text{-MCM-41}$ for nitrate anion adsorption at different initial concentrations are listed in Table3. The value of q_{Th} increased as the initial concentration increased from 50 to 100 mg/L, but k_{Th} decreased from 1.747 to 1.366. Yan model enables the anticipation of the breakthrough curve, in the entire range of outlet concentration and at time zero, furthermore, this model fixes inaccuracy results when utilization of the Thomas model, even though the high coefficient of determination was gained [16, 18]. The Yan model constants (R^2 , k_y , q_y) acquired by the nonlinear regression of the determination are more than the constant of Thomas model in all cases and arithmetically they were more important as exhibited in Table3. At all initial concentrations inspected the breakthrough response was fitted well with both models (depending on the R^2 value). Additionally, the maximum adsorption capacity (q_y) anticipated by the Yan model demonstrated a similar pattern anticipated by the Thomas model.

It can be reasoned that Yan model can be well-described the NO_3^- adsorption using $\text{NH}_2\text{-MCM-41}$ because of the high regression coefficient of determination and near q_e of experimental value and q_y in each of the three initial concentrations.

Table3: The breakthrough variables + Thomas and Yan models constants for NO₃⁻ anion in fixed bed.

Column condition			Breakthrough analysis		Thomas model		Yan model		
L (cm)	Q (ml/min)	conc. (mg/l)	q _{exp} (mg/g)	q _{th} (mg/g)	K _{th} (ml/mg.min)	R ²	q _y (mg/g)	a (min ⁻¹)	R ²
3	1.5	50	9.5377	9.6345	1.747	0.901	9.8828	16.076	0.924
3	1.5	75	10.8152	11.0266	1.446	0.923	11.2470	13.451	0.961
3	1.5	100	12.7244	14.2864	1.366	0.918	13.2514	10.715	0.95

6. Conclusions

With increasing bed height the breakthrough time increases as well as the exhaustion time, but both of them decreased with increasing NO₃⁻ inlet concentration and flow rate. Based on this study NH₂-MCM-41 offers efficient removal nitrate anion from aqueous solution in comparison with traditional activated carbon. When the bed height increases from 0.5 to 1gm, the percentage of removal increased, whereas the removal efficiency and adsorption capacity decreased acceptably with an increase in the flow rate. Also the highest bed capacity and removal percentage achieved at inlet concentration of 100mg /L of NO₃⁻ anion. Thomas and Yan adsorption models showed a good fit to the experimental data.

References

- [1] D. Majumdar & N. Gupta, "Nitrate pollution of groundwater and associated human health disorders," *Indian Journal of Environmental Health*, 42, 1, pp. 28-39, 2000.
- [2] V.C. Taty-Costodes, H. Fauduet, C. Porte, & Y.S. Ho, "Removal of lead (II) ions from synthetic and real effluents using immobilized *Pinus sylvestris* sawdust : Adsorption on a fixed-bed column," *Journal of hazardous materials*, 123, 1-3, pp.135-144, 2005.
- [3] M.H. Ward, "Workgroup report: drinking-water nitrate and health—recent findings and research needs," *Environmental health perspectives*, 113, 11, pp.1607, 2005.
- [4] M.F. Chislock, E. Doster, R.A. Zitomer, & A.E. Wilson, "Eutrophication: causes, consequences, and controls in aquatic ecosystems," *Nature Education Knowledge*, 4, 4, pp.10, 2013.
- [5] World Health Organization, "Revisions of the WHO Guidelines for Drinking Water Quality Report on a WHO Consultation," WHO Regional Office for Europe, Medmenham, UK, 1992.
- [6] Y. Cengeloglu, A. Tor, M. Ersoz, & G. Arslan, "Removal of nitrate from aqueous solution by using red mud," *Separation and Purification Technology*, 51, 3, pp.374-378, 2006.
- [7] K. Abe, A. Imamaki, & M. Hirano, "Removal of nitrate, nitrite, ammonium and phosphate ions from water by the aerial microalga *Trentepohlia aurea*," *Journal of Applied phycology*, 14, 2, pp.129-134, 2002.
- [8] S. De, & A. Maiti, "Arsenic removal from contaminated groundwater," *The Energy and Resources Institute (TERI)*, 2012.
- [9] L. Schipper, F. Unander, S. Murtishaw, & M. Ting, "Indicators of energy use and carbon emissions: explaining the energy economy link," *Annual Review of Energy and the Environment*, 26, 1, pp.49-81, 2001.
- [10] A. Elmidaoui, F. Elhannouni, M. M. Sahli, L. Chay, H. Elabbassi, M. Hafsi, & D. Largeau, "Pollution of nitrate in Moroccan ground water: removal by electrodialysis," *Desalination*, 136, 1-3, pp.325-332, 2001.
- [11] A. Bhatnagar, M. Ji, Y.H. Choi, W. Jung, S.H. Lee, S.J. Kim, & S.H. Kim, "Removal of nitrate from water by adsorption onto zinc chloride treated activated carbon," *Separation Science and Technology*, 43, 4, pp.886-907, 2008.
- [12] M. Suzukl, "Adsorption Engineering," 25, pp.2-5, 1990.
- [13] V. Batu, "Applied flow and solute transport modeling in aquifers: fundamental principles and analytical and numerical methods," *CRC Press*, 2005.
- [14] S.P. Dubey, A.D. Dwivedi, C. Lee, Y.N. Kwon, M. Sillanpaa, & L.Q. Ma, "Raspberry derived mesoporous carbon-tubules and fixed-bed adsorption of pharmaceutical drugs," *Journal of Industrial and Engineering Chemistry*, 20, 3, pp.1126-1132, 2014.
- [15] Z. Aksu & F. Gönen, "Bio sorption of phenol by immobilized activated sludge in a continuous packed bed: prediction of breakthrough curves," *Process Biochemistry* 39, 5, pp.599-613, 2004.
- [16] G. Yan, T. Viraraghavan, & M. Chen, "A new model for heavy metal removal in a biosorption column," *Adsorption Science & Technology*, 19, 1, pp.25-43, 2001.
- [17] A. Anaam & S. Noor, "Preparation of amino-functionalized mesoporous silica (MCM-41) for Nitrate anion adsorption from aqueous solution", *Journal of the Association of Arab Universities for Engineering Studies*, 4, 2019.
- [18] D. Pokhrel, & T. Viraraghavan, "Arsenic removal in an iron oxide coated fungal biomass column: analysis of breakthrough curves," *Bioresour Techno*, 99, 6, pp.2067-2071, 2008.